Power Gearbox Modelling and Dynamic Simulation of a Geared Turbofan

Haixu Wang, Yixiong Liu, Xiaolong Zhao, and Da Mo

Abstract This paper aims at the investigation of the vibration mechanism and dynamic response of the power gearbox using the established gear transmission system model. A comprehensive scheme was built consisting of modeling, assembling, boundary settings and loading to assess the deformation and vibration characteristics of the gearbox. Meanwhile, the transmission errors were included in the model to consider the effects of system errors, surface modification and manufacturing errors. Afterwards, the three –dimensional (3D) model was launched in Romax software to study the static and vibratory characteristics of the gearbox system. In addition, the meshing stiffness and transmission errors were analyzed. Finally, the gear surface modification and optimization were carried out to achieve the optimal stress distribution and reduce the maximum contact stress. The simulation results show that the maximum first mode acceleration response within the operating range was 8 g by setting the sensor at the planet wheel shaft pin. Meanwhile, the estimated transmission errors ranged from 0.13 ~ 0.15 μm. The maximum load for the planet roller bearing was 2933 N and would generate 1219 MPa contact stress, which was reasonable and acceptable. Nevertheless, the contact patch was unevenly distributed under the high-load conditions. To be specific, the maximum stress was 419 MPa locating at the gear surface edge, posing a failure risk. By performing the surface modification, the maximum stress has significantly dropped to 202 MPa and the corresponding region has moved from the edge to the surface center. The results has highlighted the importance of the proposed GTF gearbox system dynamic simulation scheme and generate a applicable approach for the transmission system engineering design.

Keywords Acceleration · Deformation · Contact stress · Surface modification · Transmission error

H. Wang · Y. Liu · D. Mo (✉)
AECC Shenyang Engine Research Institute, Shenyang 110015, China
e-mail: dada1204@126.com

X. Zhao
Romax Technology Limited, Beijing 100022, China

S. Lee et al. (eds.), *The Proceedings of the 2021 Asia-Pacific International Symposium on Aerospace Technology (APISAT 2021), Volume 2*, Lecture Notes in Electrical Engineering 913, https://doi.org/10.1007/978-981-19-2635-8_93

1 Introduction

In recent years, the stringent environmental guidelines and fierce competitions in aviation market have called for a high-fuel-efficiency, low-emission and light-weight engine for civil aircrafts [1]. Geared turbofan (GTF) engine highlights the employment of a power gearbox to link the fan and low-pressure turbine (LPT), providing an optimum rotatory speed for each component. Consequently, the fan diameter could be larger without worrying about issues including the tip speed or the structural integrity. Moreover, a higher bypass ratio (BPR) could be utilized to improve the propulsive efficiency and save fuel [2, 3]. Pratt & Whitney introduced a five-planet star system with a single-stage star epicyclic gear. The gearbox system is estimated to be reliable for at least 20 years, with an efficiency reaching 99.5% [4]. However, the gearbox system is complex and comprises of a sun gear, a planetary gear, a shaft and bearings. The sophisticated structure, limited space and complex excitation have posed critical parameters on dynamic response for the gearbox system. Therefore, the dynamic response and static stress of the fan-drive gear system have to be carefully examined to ensure safety operation.

Wang [5] proposed an improved nonlinear dynamic model of GTF gearbox, in which the structure-based time-varying gear meshing parameters and multiple nonlinear clearances were fully considered, including time-varying meshing stiffness, pressure angle, contact ratio, position angle and dynamic gear reaction force. The time-domain and frequency-domain results were investigated in terms of the dynamic response. Kang [6] studied the dynamic characteristics of double helical gear pairs both experimentally and theoretically. A set of double helical gear test devices composed of testing machines and specimens were developed, which were used to operate the double helical gear pair in the range of actual torque and rotational speed. A new type of three-piece double helical gear pair was developed for gear tests, which can realize the adjustable staggered angle from right to left. The measurement system of transmission error of three-dimensional vibration motions and dynamic motions under the condition of a high speed was realized. Mo [7, 8] analyzed the problem of multiple load distribution among star gears in a two-stage aero-engine star gear transmission system. Meanwhile, meshing errors of gear parts in a star gear transmission system were investigated, such as eccentricity error, tooth thickness error, base pitch error, assembly error and bearing manufacturing error. Furthermore, Mo [9] studied the equivalent meshing errors of different types of gear errors of the outer and the internal meshing line of the star gear transmission system respectively. A refined dynamic model was established for the analysis of vibration and natural characteristics of double helix star gear transmission system. The gear transmission system of an aero-engine was studied and calculated, meanwhile the validity of the dynamic model was verified. Chen [10] established the multi-body dynamics model of a single-stage planetary-gear rigid-flexible coupling system through ADAMS software, in which the sun gear was a flexible body, on which cracks of different sizes were established. The influence of crack parameters on the dynamic response of the planetary gear system was also analyzed. Guo

[11] improved Chen's model and established a two-stage planetary gear system. The results show that the response-side band and root mean square were sensitive to the crack fault degree of the gear pair. Other researchers have performed some investigation on the surface modification [12–15].

In this paper, the modelling, static analysis and dynamic analysis process was established for the gearbox system through the Romax software. A simulation is performed based on Hertz contact theory and dynamic characteristics of the gear system. Contact stress, system deformation, transmission error and meshing stiffness were obtained during the simulation. Furthermore, a surface modification was carried out to achieve the optimum stress distribution.

2 Methodology

2.1 Design Process

The design process of the power gearbox modelling and simulation is depicted in Fig. 1. The first is to identify the requirements for engines and build an initial model. However, due to the complexity of the gearbox system, the model is simplified with the main characteristics kept. Afterwards, the boundary conditions including

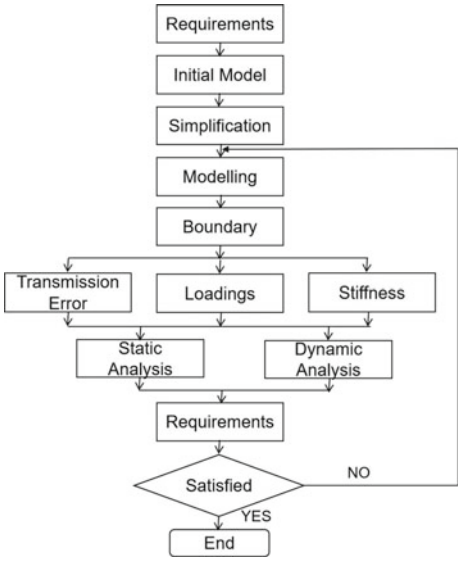

Fig. 1 Design framework

rotational speed, power, duration and stiffness are implemented to guarantee a high-fidelity and accurate simulation. Then, the static and dynamic analysis is carried out to investigate the performance and feasibility of the gearbox system.

2.2 Modelling

It is well-established that the gearbox system is complex and sophisticated, especially the hollow wall and the transmission system. The kinetic response is significantly affected by the above structures. Meanwhile, the planetary gear transmission system proves to be one of the most accessible and reliable systems for GTF engines. In this scenario, the model established is presented in Fig. 2, in which the planetary gear system is used to cater to the increasing demand for power transmission. The output shaft, inner gear ring, outer gear ring, sun gear and input shaft have been considered in the model. To be specific, 5-way herringbone gears are adopted in the model with the sun gear connected to the input shaft. Meanwhile, the output shaft is linked to the inner gear ring. After that, the planetary gears are designed in detail including the teeth number, modulus and teeth width. The model deliberated is depicted in Fig. 3. Finally, a 3-D gearbox model is launched based on the CADFUSION module through Romax software, as is shown in Fig. 4. It should be noted that in order to precisely simulate the dynamic behavior of the gearbox system, four stiffness bearings are employed at the input and output shaft, as is demonstrated in Fig. 4.

Afterwards, the boundary conditions, such as the rotation speed, power, working duration and temperature, are implemented on the model, as is listed in Table 1. The

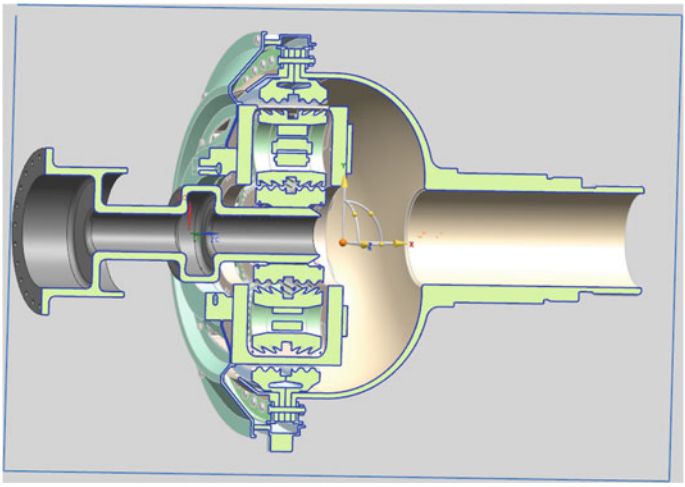

Fig. 2 Simplified planetary gear transmission system

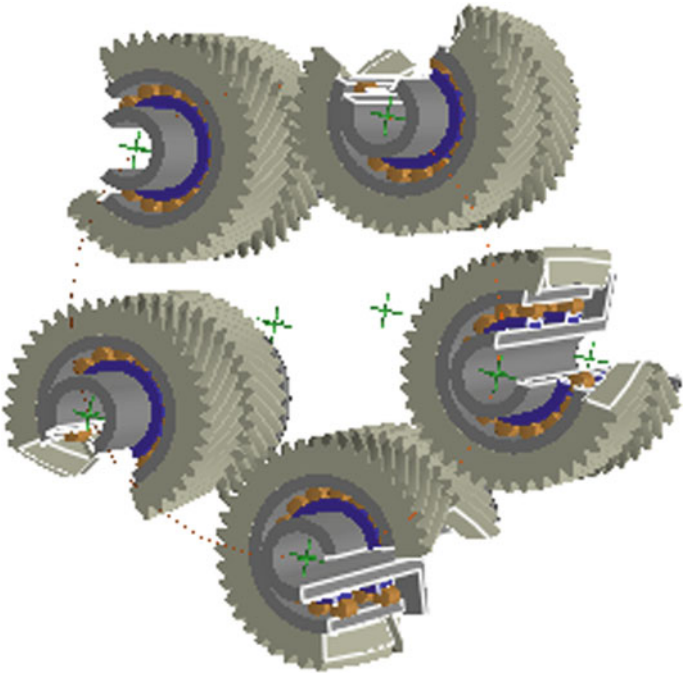

Fig. 3 Detailed planetary gear model

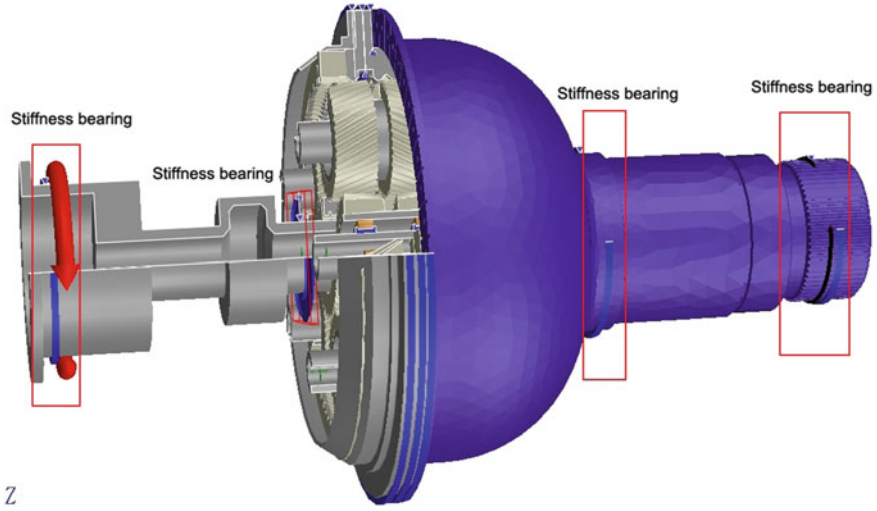

Fig. 4 Gearbox simulation model

Table 1 Boundary conditions

Loading	Value
Rotation speed (rpm)	7000
Power (kW)	3000
Duration (s)	100
Temperature (K)	343

design point speed of the input shaft is 7000 rpm and the maximum temperature is 343 K.

2.3 Contact Stress Estimation

Typically, the planetary gear transmission system is considered as multiple pairs of gears meshing and coupling with each other. Hence, the methods of static strength calculation and contact stress estimation are quite similar to those of the ordinary gears. The equation utilized for calculating the contact stress is as follows:

$$\sigma_H = Z_H Z_B Z_E Z_\varepsilon Z_\beta \sqrt{\frac{F_t}{d_p b} \frac{u+1}{u}} K_Z K_\gamma K_V K_{H\alpha} K_{H\beta} \sigma_H \sigma_H \tag{1}$$

where
F_t is the nominal tangential force of the at reference circle.
d_p is the pitch diameter of the small gear.
b is the working tooth width.
u is the gear ratio.
Z and K are the correction coefficient.

2.4 Kinetic Equation

The dynamic performance is obtained using the structural dynamic equation considering the external excitation force, as listed in (2).

$$m\ddot{x} + c\dot{x} + kx = F(t) \tag{2}$$

where
m is the mass matrix of the gear system.
k is the stiffness matrix of the gear system.
c is the damping term of the gear system.

F(t) is the excitation force.

However, with regard to the external force, it mainly comes from the gear meshing stiffness and transmission error and might exert unexpected vibration. Therefore, (2) is rearranged as (3) using the meshing stiffness and transmission error.

$$m\ddot{x} + c\dot{x} + kx = ke \tag{3}$$

where

ke is the meshing stiffness and transmission error of the gear system.

2.5 *Definition of Transmission Error*

Theoretically, the gear ratio maintains at a constant value and provides a stable and accurate reduction of rotational speed for the two gears, as is depicted in Fig. 5. However, regarding the gear deformation, manufacturing errors and surface modification, the rotation speed of the drive is not always at an expected value and there exists certain fluctuations, as is shown in Fig. 5. More importantly, the transmission error resulted would pose a fundamental excitation on the gear system and generate a significant response. As can be seen in Fig. 6, θ_2' is the real rotational angle of the driven gear, which equals to the theoretic rotational angle θ_2' plus the difference. The

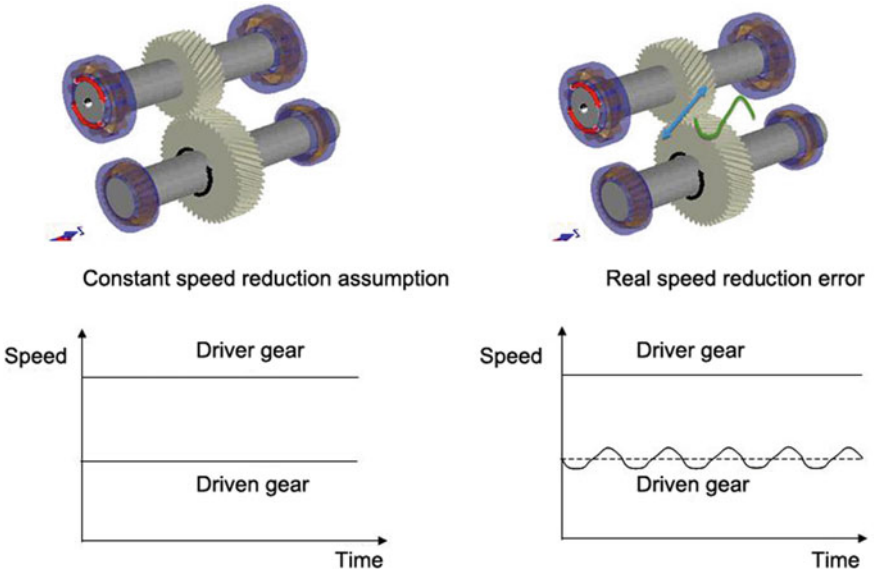

Fig. 5 Indication of transmission error

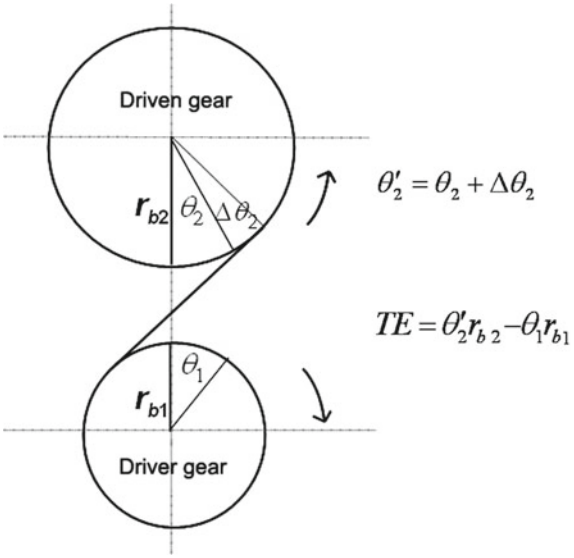

Fig. 6 Transmission error calculation

transmission error is then defined as the rotational arc length of the driven gear and the driver, as is shown in Fig. 6.

3 Results and Analysis

3.1 Static Analysis

It is of great importance to investigate the deformation and contact stress of the gearbox system to ensure a feasible engine. The total deformation distribution of the gear system is depicted in Fig. 7. One observation is that the maximum deformation occurs at the sun-planetary connecting region, reaching 0.44 μm. As shown in Fig. 8, the maximum gear dislocation reaches 4.5 μm while the minimum dislocation is only 1.67 μm.

The contact stress result of the planetary bearing roller is depicted in Fig. 9. What is interesting is that the contact stress mainly concentrates on the region whose degree is 225 to 325 with the maximum stress reaching 1219 MPa. The maximum stress lies in the degree of 275 and the corresponding load is 2933 N. Furthermore, the contact stress demonstrates an arch pattern along the distance. The maximum stress occurs at the position that is about 10 mm away from the roller.

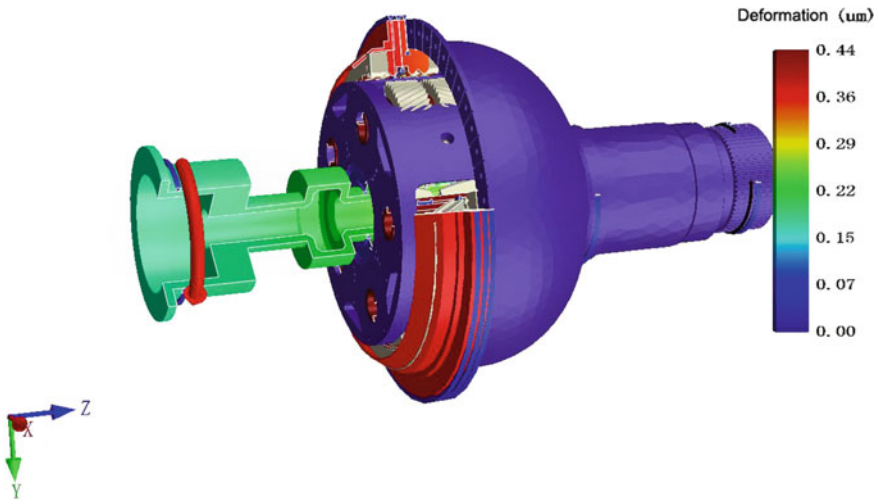

Fig. 7 Gearbox system deformation

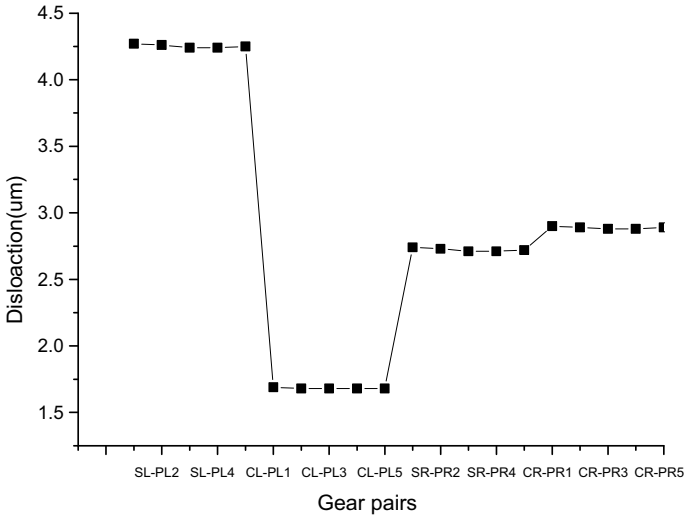

Fig. 8 Gear dislocation

3.2 Transmission Error and Meshing Stiffness

The analysis results of transmission errors have been presented in Fig. 10. The first-order transmission error ranks the highest with the range lying between 0.13 ~ 0.15 μm. However, the second- and third-order transmission errors almost reach 0. When it comes to the meshing stiffness, the results of sun gear R and the planetary gear

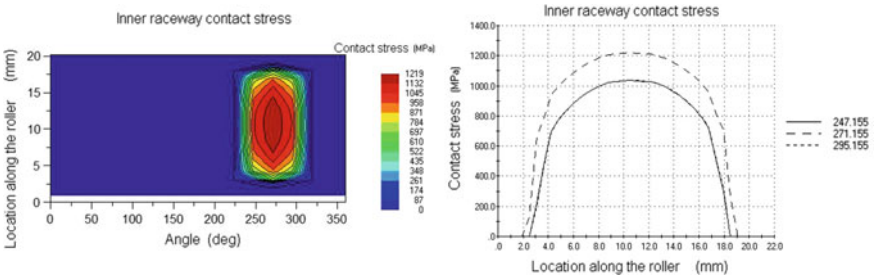

Fig. 9 Contact stress distribution

Transmission error					
First order		Second order		Third order	
Value(um)	Phase(deg)	Value(um)	Phase(deg)	Value(um)	Phase(deg)
0.13896	104.119	2.5105e-2	120.305	1.809e-3	-154.410
0.13925	176.353	2.4914e-2	-97.270	4.1601e-4	51.049
0.13872	-111.755	2.4149e-2	48.043	8.6461e-4	-53.088
0.13872	-39.879	2.4272e-2	-166.631	1.7305e-3	158.384
0.13928	31.898	2.5405e-2	-22.105	2.7698e-3	1.640
0.14105	93.925	1.2909e-2	-127.390	9.8402e-4	-68.772
0.14129	165.912	1.2681e-2	19.950	5.7435e-4	155.536
0.14108	-121.929	1.3083e-2	163.731	1.0778e-3	60.348
0.14137	-49.784	1.4039e-2	-53.636	1.919e-3	-85.175
0.14119	22.024	1.3534e-2	88.014	1.4124e-3	99.696
0.13561	124.394	9.8768e-3	58.919	1.0836e-3	34.699
0.13565	-163.871	9.8025e-3	-154.943	9.6716e-4	174.738
0.13567	-91.934	9.8952e-3	-10.285	6.8922e-4	-12.894
0.13543	-19.618	1.0024e-2	130.544	5.9465e-4	30.323
0.1361	52.645	1.0191e-2	-87.759	1.8007e-3	-137.324
0.14015	117.663	1.2174e-2	-1.589	1.7885e-3	50.748
0.14098	-170.157	1.2627e-2	141.390	2.7948e-3	-91.443
0.1407	-98.406	1.229e-2	-73.091	2.2125e-3	100.420
0.14095	-26.671	1.221e-2	72.482	1.5782e-3	-77.079
0.14019	45.420	1.1948e-2	-144.466	1.1329e-3	169.966

Fig. 10 Transmission error distribution

R1 are shown in Fig. 11. It is clear that the conjugate stiffness maintains a constant value at 20 GPa. Nevertheless, the sun gear and the planetary gear present a contradictory trend. As the rolling angle increases, the stiffness of the sun gear linearly drops from 72 to 21 GPa, whereas the stiffness of the planetary gear increases from 21 to 72 GPa.

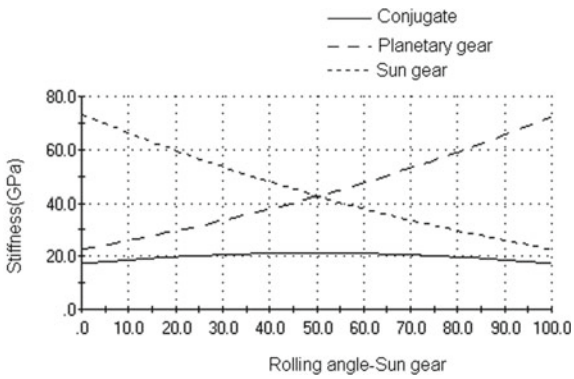

Fig. 11 Meshing stiffness

3.3 Dynamic Simulation Results

In order to precisely simulate the dynamic performance of the gearbox system and obtain the response of the system, five acceleration measuring points were implemented on the planetary gear pin, as is shown in Fig. 12. The first-order response of components X, Y and Z as well as the total response are described in Fig. 13. Apparently, the maximum response of the planetary pin occurs at a rotational speed ranging from 2000 to 3000 rpm. At this time, the component X accounts for the largest response, peaking 7.5 g, while the total response is 8 ms^{-2}. A closer inspection on the figure shows that at 4000 to 5000 rpm, the response of Component Z is the most influential factor, approaching 5.6 ms^{-2}. Furthermore, the response of Component Y is relatively low for the whole simulation.

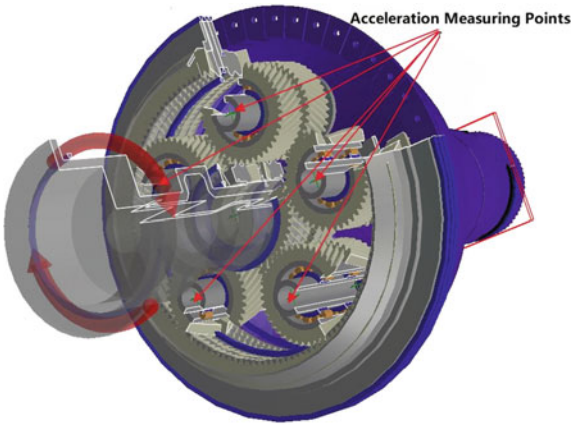

Fig. 12 Acceleration measuring points

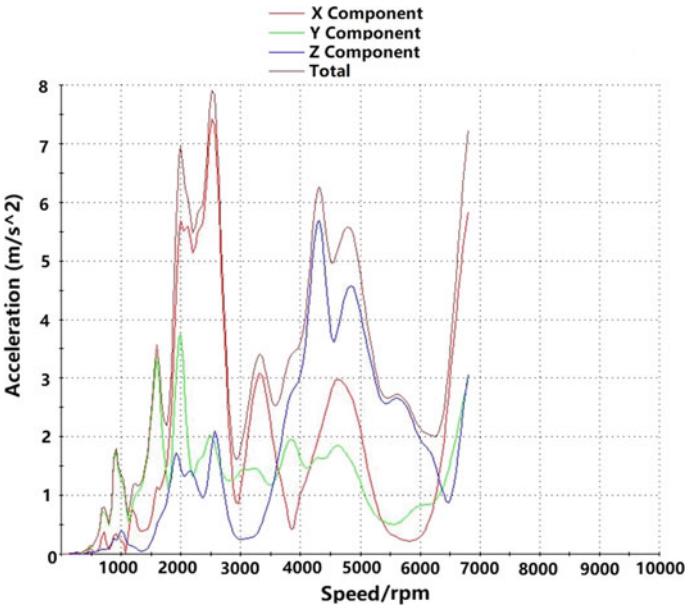

Fig. 13 Planetary pin acceleration response of measuring point 1

Afterwards, the system acceleration response and deformation at the point with the maximum planetary pin response are depicted in Figs. 14 and 15. Obviously, the planetary gears play a crucial role in system dynamic response. The meshing of

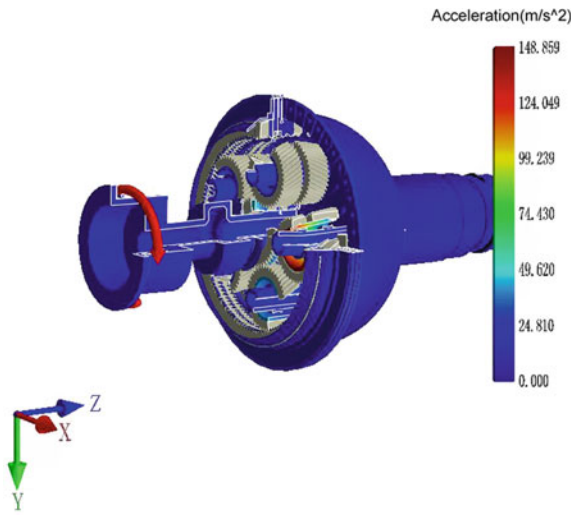

Fig. 14 System acceleration response at 2600 rpm

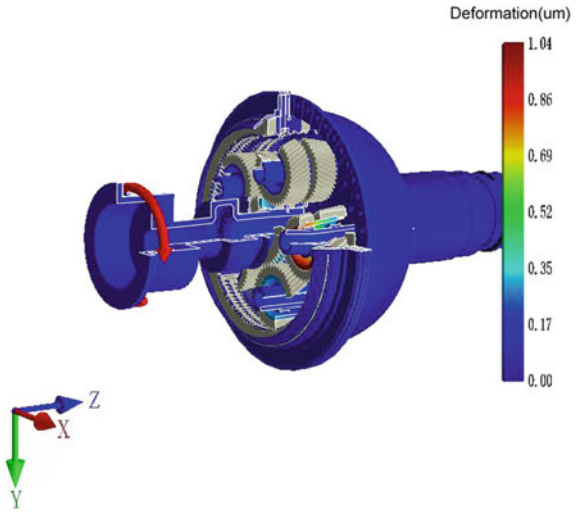

Fig. 15 System deformation at 2600 rpm

the gears has resulted in a system response and deformation of 149 ms^{-2} and 1.04 um respectively, which highlights the importance of thorough consideration on the mitigation of the external excitation.

3.4 Surface Modification

The contact stress between the sun gear and the planetary gear surface is depicted in Fig. 16. One observation is that the large-stress area locates at the edge, reaching 419 MPa. Moreover, there exists an uneven contact since the low-stress region lies on the other edge, indicating a partial load condition and a failure risk, especially

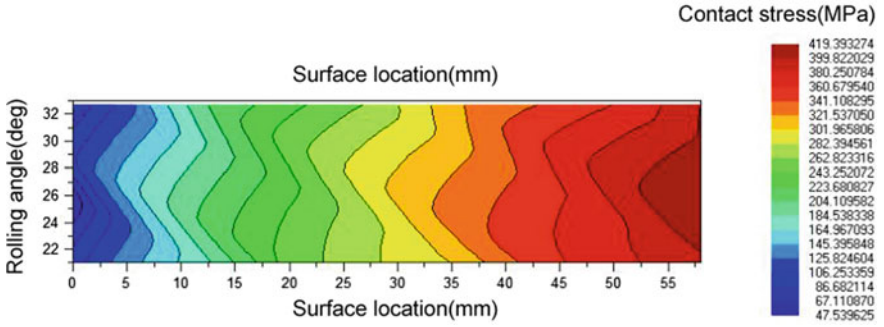

Fig. 16 Contact stress spots distribution

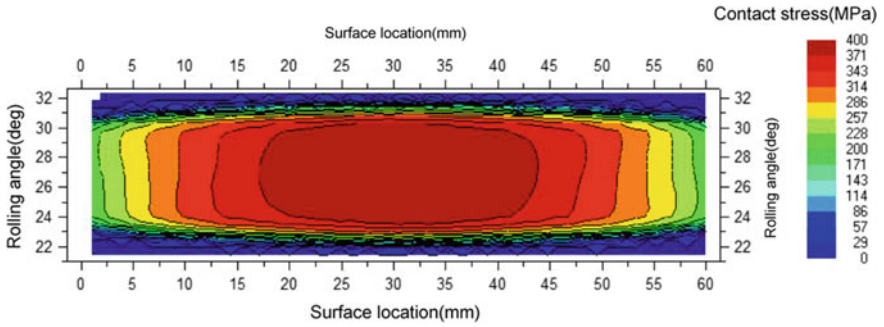

Fig. 17 Contact stress spots distribution after optimization

under the heave loading condition. Therefore, it is necessary to perform a surface modification to eliminate the uneven contact.

A design optimization is carried out in Romax aiming at improving the contact condition and reduce the transmission error. By optimizing parameters of the sun gear and planetary gear, the optimal contact spot is located in the central area of the tooth surface, as is shown in Fig. 17. The maximum contact stress is 400 MPa, which is 19 MPa lower than the previous design. More importantly, the edge stress has dropped from 419 to 217 MPa and the gear failure risk has been dramatically reduced.

4 Conclusion

This paper performs a systematic study on the gearbox system static and dynamic response. A design process has been established including modeling, boundary conditions, static and dynamic analysis, surface modification. The main conclusions are concluded as follows:

1. The maximum contact stress of the planetary gear bearing roller is 1219 MPa and the corresponding force is 2933 N. Meanwhile, the maximum deformation of the gear system is 0.44 μm whereas the dislocation value of the sun-planetary gear reaches 4.27 μm due to the uneven contact.
2. The transmission error of the investigated gear system is 0.13 to 0.15 μm while the meshing stiffness approaches 72 GPa. Consequently, the generated maximum acceleration response for the planetary shaft pin and the gear system is 8 and 149 ms^{-2} respectively.
3. The existing uneven contact has resulted in 417 MPa contact stress at the tooth surface edge. After optimization, the optimal stress falls to 400 MPa while the edge stress is only 217 MPa. It highlight the importance of surface modification to reduce the possible gear failure.

Acknowledgements The authors would like to thank AECC Shenyang Engine Research Institute for the fund and support.

References

1. Realising Europe's vision for aviation, Strategic Research & Innovation Agenda (2012) ACARE. http://www.acare4europe.org/sites/acare4europe.org/files/attachment/SRIA%20Volume%201.pdf
2. Mo D (2021) Conceptual design of a two-shaft high bypass turbofan engine for entry-into-service 2025. MSc thesis, Cranfield University
3. Liu YX (2021) Optimization of hybrid electric propulsion system. MSc thesis, Cranfield University
4. Pratt & Whitney (2015) The Pratt & Whitney PurePower ® Geared Turbofan TM Engine. https://academieairespace.com/wp-content/uploads/2018/05/prattw.pdf
5. Wang S, Zhu R (2021) Theoretical investigation of the improved nonlinear dynamic model for star gearing system in GTF gearbox based on dynamic meshing parameters. Mech Mach Theory 156:104–108
6. Kang MR, Kahraman A (2015) An experimental and theoretical study of the dynamic behavior of double-helical gear sets. J Sound Vib 350:11–29
7. Mo S, Yidu Z, Qiong W (2015) Research on multiple-split load sharing of two-stage star gearing system in consideration of displacement compatibility. Mech Mach Theory 88:1–15
8. Mo S, Zhang Y, Wu Q et al (2016) Research on natural characteristics of double-helical star gearing system for GTF aero-engine. Mech Mach Theory 106:166–189
9. Mo S, Zhang T, Jin GG et al (2020) Analytical investigation on load sharing characteristics of herringbone planetary gear train with flexible support and floating sun gear. Mech Mach Theory 144:103670
10. Chen C, Guo W, Huang LJ (2016) A rigid-flexible coupled model for a planetary gearbox with tooth crack and its dynamic response analyses. 2016 Prognostics and System Health Management Conference (PHM-Chengdu), Chengdu, China
11. Guo W, Chen C, Xiao N (2018) Dynamic vibration feature analyses for a two-stage planetary gearbox with a varying crack using a rigid-flexible coupled model. J Intel Fuzzy Syst 34(6):3869–3880
12. Zhao HX, He L, Meng JB, Wu XZ, Ju GQ, Sun HB (2019) Topology modification and simulation of herringbone gear based on Romax. Coal Mine Mach 1(1):158–161
13. Lin J, Parker RG (1999) Analytical characterization of the unique properties of planetary gear free vibration. J Vib Acoust 121(3):316–321
14. Cao JF, Chen ZG, Chen SY, Tang JY (2017) Analysis of the effect of shaft angle on dynamic characteristic of the split torque transmission system with herringbone gear. J Mech Trans 41(8):94–99
15. Liu C, Fang Z, Feng W (2018) An improved model for dynamic analysis of a double-helical gear reduction unit by hybrid user-defined elements: Experimental and numerical validation. Mech Mach Theory 127:96–111